Research Article ISSN 2771-666X

Journal of Advanced Materials Science and Engineering

# Correlation Analysis and Morphological Characteristics of a PDLC Composite for Optoelectronic Applications

**Egamov Mukhtor[1,3], Makhsudov Barot[2], Rakhimova Umeda[1] and Yorov Maruf[1]**

[1]*Khujand Scientific Center of the National Academy of Sciences of Tajikistan.*

[2]*Tajik National University.*

[3]*Mining and Metallurgical Institute of Tajikistan.*

***Correspondence:**
Egamov Mukhtor, Khujand Scientific Center of the National Academy of Sciences of Tajikistan.

**Received:** 04 Jan 2026; **Accepted:** 16 Feb 2026; **Published:** 25 Feb 2026

**Citation:** Egamov Mukhtor, Makhsudov Barot, Rakhimova Umeda, et al. Correlation Analysis and Morphological Characteristics of a PDLC Composite for Optoelectronic Applications. J Adv Mater Sci Eng. 2026; 6(1): 1-6.

## ABSTRACT

*A fabrication method and the optical characteristics of a polymer-dispersed liquid crystal (PDLC) system based on polyvinyl butyral (PVB) as the polymer matrix and 4-n-pentyl-4'-cyanobiphenyl (5CB) as the liquid crystal are proposed. PDLC films were prepared using the thermal-induced phase separation (TIPS) method with various compositions of the two components. Detailed investigations employing polarized optical microscopy and differential scanning calorimetry were carried out to assess the correlation between the composite composition and PDLC formation. It was found that PVB and 4-n-pentyl-4'-cyanobiphenyl (5CB) are partially miscible, with a maximum solubility limit of 42.8%. The presented thermal results and analysis expand the current understanding of TIPS-based PDLC formation. The use of PVB as a polymer matrix in PDLC systems opens up new possibilities in PDLC design due to the superior performance of PVB compared to other polymers commonly used in PDLC systems. It is demonstrated that PVB can serve as an effective polymer matrix for the formation of PDLC systems.*

## Keywords

Polymer-dispersed liquid crystals; Polyvinyl butyral; Polarized optical microscopy; Differential scanning calorimetry.

## Introduction

Melting and mixing of monomeric and polymeric precursors are well-established approaches for the fabrication of functional materials. In recent years, significant research efforts have been directed toward the investigation of mesomorphic precursors, such as liquid crystals. An important practical application of these studies is represented by polymer-dispersed liquid crystals (PDLC) fabricated via polymerization-induced phase separation (PIPS). PDLC constitute a novel class of materials that are highly promising for applications in switchable (smart) windows and projection display technologies [1–4]. The potential implementation of PDLC films as optical information storage media [5] or as capacitors in reliable microscale energy-harvesting systems [6] further enhances the attractiveness of these materials. Typically, PDLC systems consist of liquid crystal (LC) droplets dispersed within a solid polymer matrix. These micron-sized droplets (about 3–25 μm) are responsible for the unique functional properties of the material. By controlling the orientation of LC molecules through the application of an external electric field, the intensity of transmitted light can be effectively modulated. A key advantage of PDLC materials is the relative simplicity of their fabrication process. They have been fabricated using various techniques, including encapsulation (emulsification) and phase separation, with the latter becoming the predominant production method [7-9]. The simplest approach to producing PDLC materials involves cooling from a homogeneous mixture of a liquid crystal and a thermoplastic polymer. The performance of PDLC systems is strongly dependent on the final morphology of the dispersed LC domains within the polymer matrix. The size, shape, and spatial distribution of the LC domains are governed not only by thermodynamic phase equilibrium but also depend critically on the types of polymers and liquid crystals employed, as well as on interfacial interactions [7,8]. It has been found that the electro-optical properties of PDLC systems vary significantly depending on the choice of constituent materials.

The polymer, as a key component of PDLCs, exerts a substantial influence on their electro-optical performance. Various polymer matrices have been employed in PDLC systems, including polystyrene (PS), polymethyl methacrylate (PMMA), polyacrylate (PA), polyvinyl alcohol (PVA), and the UV-curable resin NOA65 (Norland Products, Cranbury, New Jersey, USA) [10-13].

Among the polymers listed above, another thermoplastic material—polyvinyl butyral (PVB)—has attracted attention, as its use as a component in composite formulations may play a significant role in the development of high-performance materials with tailored properties [14,15]. In this work, we investigate the formation of PDLC systems employing PVB as the polymer matrix.

This article describes the preparation and thermotropic characteristics of a liquid crystal composite based on the nematic liquid crystal (NLC) 4-n-pentyl-4′-cyanobiphenyl (5CB) and polyvinyl butyral (PVB) as the polymer matrix. PDLC samples were fabricated using the thermal-induced phase separation (TIPS) method with various compositions of the two components. A comprehensive investigation employing polarized optical microscopy (POM) and differential scanning calorimetry (DSC) was carried out to establish the correlation between the composite composition and the morphology of the resulting films. The primary objective of the present work is the development of PDLC systems utilizing PVB as the polymer matrix, owing to its superior performance characteristics as a structural material. A rational mechanism has been devised for the fabrication of stable PDLC films suitable for optical applications.

## Experimental Section

### Polymer Matrix

Polyvinyl butyral (PVB), obtained from Merck, was selected as the polymer matrix. PVB belongs to the family of high-performance thermoplastics and is produced through the reaction of acetylated polyvinyl alcohol with butyraldehyde. The backbone of the polymer chain is derived from the polyvinyl alcohol chain, but without hydroxyl substituents: during the polymer-analogous transformation, hydroxyl groups react with protonated butyral dehyde molecules, resulting in the formation of a fundamentally new polymer structure.

PVB is a semi-rigid polymer with a linear chain structure, characterized by high mechanical strength, the highest service temperature among melt-processable thermoplastics, low creep, good electrical properties, optical transparency, and resistance to lubricants, many solvents, and chemicals. Its elevated thermal stability is particularly advantageous for electronic applications, including exposure to vapor phases or infrared soldering temperatures. Importantly, PVB retains these properties within the temperature range of 100 °C to 150 °C. Moreover, it exhibits high chemical resistance to mineral acids, alkalis, and electrolytes across a pH range of 2 to 13. It is resistant to oxidizing agents, allowing for cleaning with bleaching agents, and it also exhibits stability against surfactants and hydrocarbon oils. However, it is not resistant to low-polarity organic solvents (e.g., ketones and chlorinated hydrocarbons) or aromatic hydrocarbons. Mechanically, PVB demonstrates high compressive strength, making it suitable for applications under elevated pressure. Due to its relatively low raw material and processing costs, PVB is employed in specialized applications and often serves as an excellent alternative to polycarbonates. PVB enables the facile fabrication of membranes, which can be applied in areas such as wastewater treatment, food and beverage processing, and gas separation. For the present study, we employed transparent PVB with a glass transition temperature of 58 °C, determined via DSC measurements during the first heating cycle (1 h) at a heating rate of 20 °C/min.

### Liquid crystal

As the nematic component, a single-component liquid crystal of the 4-n-pentyl-4′-cyanobiphenyl type (5CB) [16] was employed. This choice of CN-terminated liquid crystal was motivated by the chemical stability of CN-containing LCs, their short relaxation times, and high dielectric anisotropy. Such materials are widely used in liquid crystal display (LCD) technologies. The resulting mixtures were dried in a thermal oven at 50 °C for 24 hours. The structure of the NLC 5CB compound was confirmed by Fourier-transform infrared spectroscopy (FT-IR, BKFT-30), differential scanning calorimetry (DSC), and elemental analysis.

FT-IR spectra of KBr pellets were analyzed based on the following absorption bands: 3071 $cm^{-1}$ (aromatic C–H stretching), 2958–2873 $cm^{-1}$ (aliphatic C–H stretching), 2225 $cm^{-1}$ (C≡N stretching), 1622 $cm^{-1}$ (C=N stretching), 1588, 1504, 1465 $cm^{-1}$ (aromatic ring C–C stretching), 1250 $cm^{-1}$ (C–O–C stretching), and 839 $cm^{-1}$ (absorption assigned to the 1,4-phenylene ring).

The properties of NLC 5CB were further verified using polarized optical microscopy (POM) and DSC.

### Preparation of PDLC Films

PDLC composites were fabricated using the TIPS and SIPS techniques. NLC 5CB and PVB were mixed in various weight ratios (Table 1) and dissolved in ethanol ($C_2H_5OH$) to obtain a 5 wt.% solution.

The resulting solutions were stirred using a magnetic stirrer for 0.5 h, then poured onto glass plates and allowed to stand at room temperature for 24 h, followed by drying in a constant-temperature drying oven (BOV-T70C) for 24 h to remove the solvent.

**Table 1:** Compositions used for PDLC preparation.

| Code | P1N9 | P2N8 | P3N7 | P4N6 | P5N5 | P6N4 | P7N3 | P8N2 | P9N1 |
|---|---|---|---|---|---|---|---|---|---|
| PVB | 10 | 20 | 30 | 40 | 50 | 60 | 70 | 80 | 90 |
| 5CB | 90 | 80 | 70 | 60 | 50 | 40 | 30 | 20 | 10 |

To prepare PDLC films via the PIPS method, the films were heated to 80 °C (above the $T_g$ of PVB) at a heating rate of 20 °C/min to ensure thorough mixing, followed by cooling at a rate of 10 °C/min. In this manner, well-defined PDLC films were obtained for the specific mixture compositions, and their formation was monitored using polarized optical microscopy (POM) [11].

## Experimental Methods

DSC thermograms were recorded during heating–cooling cycles at a heating rate of 20 °C/min and a cooling rate of 10 °C/min over the temperature range of 20–180 °C. Measurements were performed using a Netzsch differential scanning calorimeter (DSC BK-DSC 300L) under a nitrogen atmosphere. Glass transition temperatures ($T_g$) were determined as the midpoint of the step change in the baseline, while peak maxima were reported as the temperatures corresponding to first-order phase transitions.

The phase behavior of NLC 5CB and the PDLC composites was further investigated using polarized optical microscopy (POM) with a POLAM-2 microscope equipped with a MYscope 500 M digital video camera (Webbers), enabling both photographic and video recording of the ongoing processes.

## Results and Discussion

Polarized optical microscopy (POM) and differential scanning calorimetry (DSC) were employed to characterize the pure components and the PDLC films. These analyses allowed for the determination of the spatial arrangement and structure of the liquid crystals within the polymer matrix. DSC measurements performed on PVB revealed a glass transition at 58 °C (Figure 1).

For 5CB, the DSC thermograms exhibit three endothermic peaks upon heating and two exothermic peaks upon cooling. According to POM observations, the DSC peaks are assigned as follows: the solid–solid transition corresponds to the first endothermic peak at 51 °C, the mesophase transition from the crystalline to the nematic phase corresponds to the second endothermic peak, and the final endothermic peak corresponds to the nematic-to-isotropic transition (Figure 1). As reported in [17], the endothermic peak associated with the crystalline-to-nematic transition exhibits a higher enthalpy change compared to the peak corresponding to the nematic-to-isotropic transition (Table 2). The weak exothermic peak corresponds to the isotropic-to-nematic transition, whereas the stronger exothermic peak represents the nematic-to-crystalline transition. During cooling, the solid–solid transition disappears. The nematic mesophase exhibits a marble-like texture upon heating and a schlieren texture with two- and four-brush patterns [18] upon cooling (Figure 2,a and 2,b), remaining stable over a wide temperature range up to 66 °C.

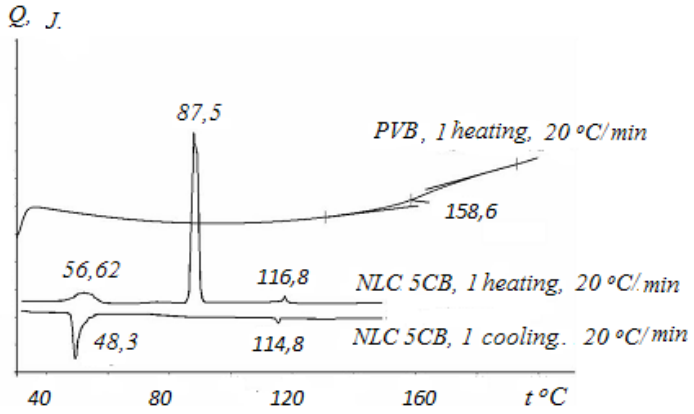


**Figure 1:** DSC thermograms for 4-n-pentyl-4'-cyanobiphenyl (5CB).

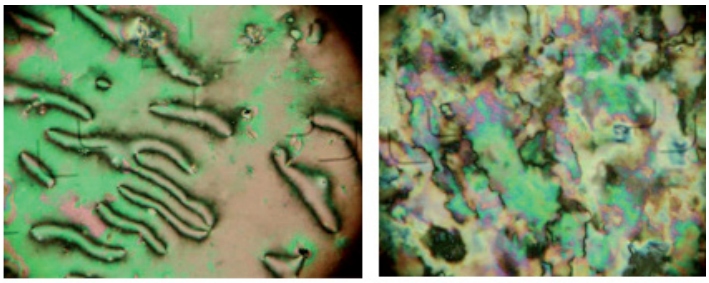


**Figure 2:** Micrographs of 5CB composites at different temperatures obtained by (*a*) polarized optical microscopy and (*b*) crossed-polarizer imaging.

**Table 2:** Thermotropic behavior of PDLC films.

| Code | $T_g$ ($T_m$ [1]) | $T_{S-S}$ (ΔH) | $T_m$ [2] (ΔH) | $T_i$ (ΔH) | $T_{Cr}$ (ΔH) | POM |
|---|---|---|---|---|---|---|
| 5CB | - | 56.62 | 87.5 | 114.78 | 48.32 | Marble and schlieren texture |
| P1N9 | - | 65.87 | 86.4 | 108.62 | 46.92 | Thermotropic behavior |
| P2N8 | - | 50.75 | 85 | 102.58 | 42.23 | Large drops when cooling |
| P3N7 | 55,1 | - | 84.3 | - | 36.37 | Small drops when cooling |
| P4N6 | 52 | - | 86.8 | - | 42.23 | Small drops when cooling |
| P5N5 | 62 | - | 86.4 | 98.4 | 39.19 | Large drops when cooling |
| P6N4 | 63 | - | 62/7 | 77.5 | - | Fine texture when first heated |
| P7N3 | 49.9 | - | 56.3 | - | - | Rarely falling drops during cooling |
| P8N2 | 82.7 | - | - | - | - | Fine texture when first heated |
| P9N1 | 104.29 | - | - | - | - | Amorphous behavior |
| PVB | 158 | - | - | - | - | Amorphous behavior |

***Notes:*** *$T_g$: glass transition temperature; $T_{1_m}$: melting temperature of the polymer matrix enriched with liquid crystals; $T_{2_m}$: melting temperature of the liquid crystal; $T_i$: isotropization temperature; $T_{Cr}$: crystallization temperature; all temperatures are given in °C. ΔH: enthalpy change, measured in J/g.*

Composites containing the highest fractions of NLC 5CB (P1N9 and P2N8) exhibit DSC traces similar to those of the pure (pristine) liquid crystal, with the primary differences being slight reductions in the melting temperatures (by 1 °C and 2 °C, respectively) and the isotropization temperatures (by 6 °C and 12 °C, respectively). This effect can be attributed to the presence of a small amount of PVB, which acts as an impurity in the system.

A more detailed analysis of the thermograms revealed that, in addition, the composites exhibit a weak exothermic peak at approximately 0 °C. POM observations show a marble-like texture for P1N9, similar to that of pure 5CB, whereas for P2N8, large droplets were observed during cooling scans (Figure 3,*a*). Based on these observations, the larger exothermic peak (around 40 °C) was attributed to the crystallization of the large droplets, while the smaller exothermic peak (around 0 °C) was assigned to the crystallization of the small droplets.

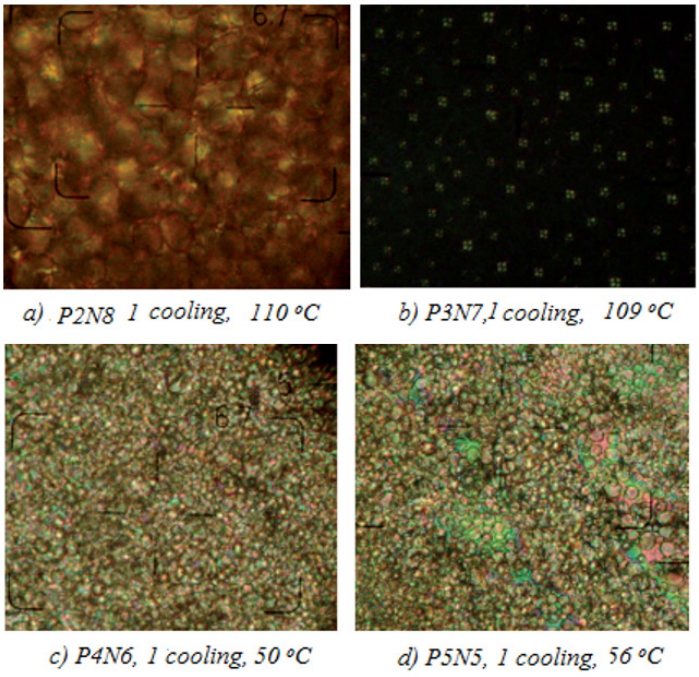


**Figure 3:** Micrographs of PDLC composites at different temperatures obtained by (*a, c*) polarized optical microscopy and (*b, d*) crossed-polarizer imaging.

Composites containing intermediate amounts of NLC 5CB (P3N7, P4N6, and P5N5) clearly exhibit phase separation upon cooling, forming small, round droplets with birefringence dispersed within the polymer matrix (Figure 3,*b–d*). Phase separation is noticeable even in the isotropic phase of 5CB under normal illumination (Figure 4,*a*). Crystallization of the nematic droplets was not observed by POM until the samples reached room temperature. DSC thermograms revealed a broad, weak peak upon heating at approximately 55 °C for P3N7, which appeared only as a faint shoulder at 62 °C for P5N5, along with an intense peak around 85 °C corresponding to the crystalline-to-nematic mesophase transition (Figure 4). The endothermic peak associated with isotropization is clearly observed only for P5N5, while for P4N6 it appears as a very weak and broad feature, and for P3N7 it is not evident during the heating scan.

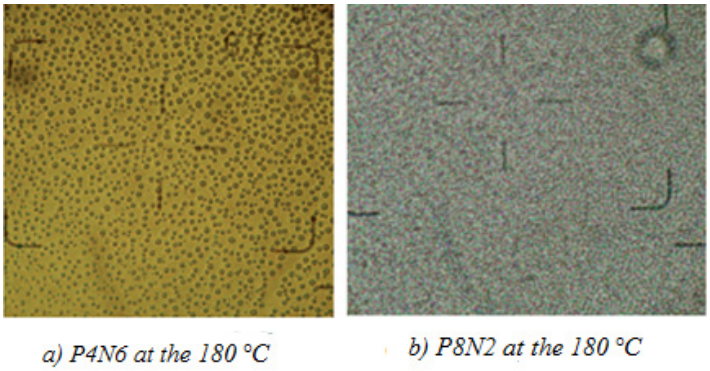


**Figure 4:** Micrographs of composites P4N6 and P8N2 at *180 °C* obtained by (*a*) polarized optical microscopy and (*b*) crossed-polarizer imaging.

During cooling scans, the peak corresponding to the phase separation temperature was not observed, likely due to the dispersion of the liquid crystal into small droplets, whose clearing-to-separation transitions occur over very short timescales. Consequently, DSC, hindering the analysis of this transition, which is necessary for determining the separation temperature, could not detect the associated enthalpy change. It is well known that this transition is accompanied by only a small enthalpy change [19].

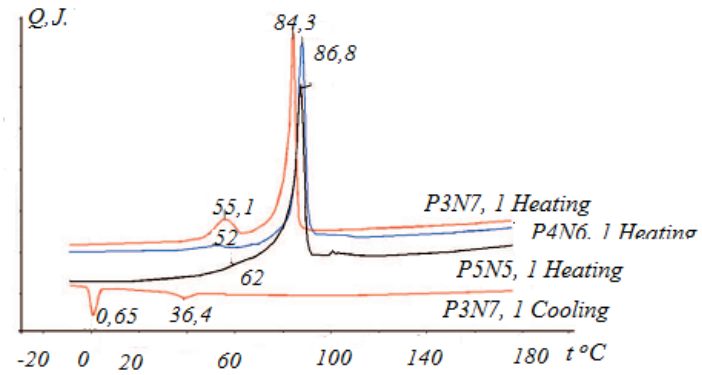


**Figure 5:** DSC traces of composites containing intermediate fractions of NLC 5CB.

Isotropization temperatures were determined from POM observations (Table 2). In the cooling images, two exothermic peaks are visible: a small peak around 40 °C and a more intense peak near 0 °C, corresponding to a two-step crystallization process due to droplets of different sizes. By comparing these results with the thermal behavior of P1N9 and P2N8, the stronger exothermic peak (0 °C) was attributed to the crystallization of the small droplets, while the weaker peak (40 °C) corresponds to the crystallization of the large droplets. The lower crystallization temperature of the small droplets indicates that the level of polymer contamination in these droplets is lower than in the large ones. By comparing the enthalpy changes of both crystallization events, it can be

concluded that increasing the polymer fraction in the composites leads to a higher density of small droplets relative to large ones. Furthermore, when comparing the enthalpy changes across all composites, a decrease in the crystallization enthalpy was observed with increasing polymer content, which likely reflects a reduction in the liquid crystal fraction within the droplets due to greater dissolution of 5CB in the polymer matrix. Under these conditions, the first endothermic peak in the DSC traces corresponds to melting (for P3N7 and P4N6) or glass transition (for P5N5–P9N1) of the liquid crystal dispersed within the polymer matrix.

For the P6N4 and P7N3 composites, the DSC thermograms exhibit two broad peaks upon heating, corresponding to the melting and isotropization of the homogeneous mixtures (Figure 6). During the cooling scan and the second heating scan in DSC, only the glass transition was observed, whereas POM during cooling revealed the presence of a few dispersed LC droplets.

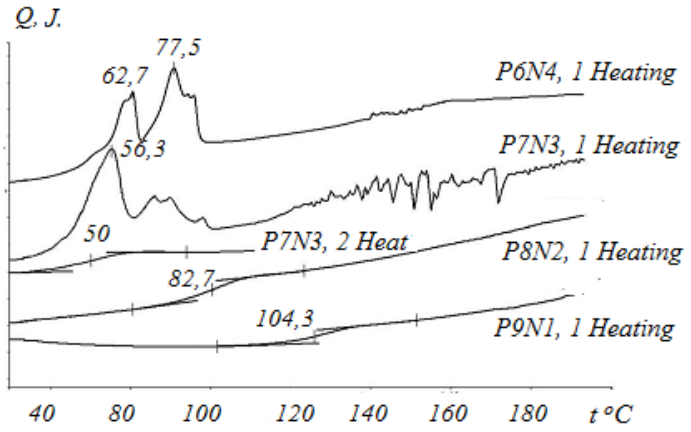


**Figure 6:** DSC curves of composites containing low fractions of NLC 5CB.

For the P8N2 and P9N1 composites, the DSC thermograms are similar to those of pure PVB. This indicates that the low 5CB content in these composites (10 % and 20 %) is insufficient to induce phase separation; the liquid crystal dissolves in the polymer and functions primarily as a plasticizer, lowering the glass transition temperature of the matrix. In POM, films prepared via the heating/cooling procedure appear isotropic under polarized light and exhibit fine granulation under normal illumination (Figure 4b). The corresponding DSC and POM data are summarized in Table 2.

By combining the DSC and POM data for the pure components and all investigated composites, it can be concluded that the process does not result in complete phase separation of the two components. A fraction of NLC 5CB inevitably remains dissolved in the polymer matrix, acting as a plasticizer and reducing the glass transition temperature of the matrix.

## Conclusions

Using the TIPS method, novel PDLC systems were prepared with PVB as the polymer matrix and the low-molecular-weight liquid crystal 5CB. POM analysis revealed the formation of well-defined liquid crystal droplets upon cooling in composites containing 70 %, 60 %, and 50 % NLC 5CB.

DSC measurements confirmed the POM observations and indicated that PVB and 4-n-pentyl-4′-cyanobiphenyl (5CB) are partially miscible, with a maximum solubility limit of 42.8 %. The presented thermal results and analysis expand the current understanding of PDLC formation via the TIPS method. The use of PVB as a polymer matrix in PDLC systems opens new opportunities in PDLC design, owing to the superior performance characteristics of PVB compared to other polymers commonly employed in PDLC systems.

## Acknowledgments

The authors express their gratitude to the Ministry of Finance of the Republic of Tajikistan for the financial support provided under Project 0121TJ1107 dated March 10, 2021.

## References

1. Drzaic PS. Liquid Crystal Dispersions. World Scientific Publishing, Singapore. 1995; 448.
2. Blinov LM, Chigrinov VG. Electrooptic effects in liquid crystal materials. Springer Nature. 1994; 464.
3. Mucha M. Polymer as an important component of blends and composites with liquid crystals. Prog in Polym Sci. 2003; 28: 837-873.
4. Dierking I. Textures of Liquid Crystals. Wiley Online Library. 2003; 230.
5. Malik P, Raina KK. Droplet orientation and optical properties of polymer dispersed liquid crystal composite films. Opt Mater. 2004; 27: 613-617.
6. Liu YJ, Ding X, Lin SCS, et al. Surface acoustic wave driven light shutters using polymer-dispersed liquid crystals. Adv Mater. 2011; 23: 1656-1659.
7. Zyryanov VYA, Krakhalev MN, Prishchepa OO, et al. Inverse regime of ionic modification of surface anchoring in nematic droplets. JETP Lett. 2008; 88: 597-601.
8. Loiko VA, Krakhalev MN, Konkolovich AV, et al. Experimental results and theoretical model to describe angular dependence of light scattering by monolayer of nematic droplets. J Quant Spectrosc and Radiat Transfer. 2016; 178: 263-268.
9. Marin L, Ailincai D, Paslaru E. Monodisperse PDLC composites generated by use of polyvinyl alcohol boric acid as matrix. RSC Adv. 2014; 4: 38397-38404.
10. Lin YH, Chu TY, Tsou YS, et al. An electrically switchable surface free energy on a liquid crystal and polymer composite film. Appl Phys Lett. 2012; 101: 233502.
11. Shih WP, Chung SY, Chen YY, et al. Tunable capacitor based on polymer-dispersed liquid crystal for power harvesting Microsystems. IEEE Trans Electron Devices. 2008; 55: 2568-2573.

12. Wang J, Xia J, Hong SW, et al. Phase separation of polymer-dispersed liquid crystals on a chemically patterned substrate. Langmuir. 2007; 23: 7411-7415.
13. Egamov M. Studies of the structure and properties of polymer dispersed liquid crystal films to create a polarizer. J of Poly Sci and Eng. 2024; 7: 8606-8614.
14. Egamov MKH, Maksudov BI, Faizulloev IKH. Optical hysteresis in composites based on polymernematic liquid crystal under uniaxial deformation. Russian Physics J. 2022; 65: 488-492.
15. Egamov M. Studies of the structure and properties of polymer dispersed liquid crystal films to create a polarizer. J Poly Sci and Eng. 2024; 7: 132-144.
16. Gray GW, Harrison KJ, Nash JA. New family of nematic liquid crystals for displays. Electron Lett. 1973; 9: 130-131.
17. Mansare T, Decressain R, Gors C, et al. Phase transformations and dynamics of 4-cyano-4′-pentylbiphenyl (5CB) by nuclear magnetic resonance, analysis differential scanning calorimetry, and wideangle x-ray diffraction analysis. Mol Cryst Liq Cryst. 2002; 382: 97-111.
18. Egamov MKH, Rakhimova UJ. Modifications of the structure of polymer-liquid crystal films for obtaining polarizers. Rep of the Natio Acad of Sci of Tajikistan. 2021; 64: 682-686.
19. Marin L, Cozan V, Bruma M. Comparative study of new thermotropic polyazomethines. Polym Adv Technol. 2006; 17: 654-672.